

Weierstraß-Institut
für Angewandte Analysis und Stochastik
Leibniz-Institut im Forschungsverbund Berlin e. V.

Preprint

ISSN 0946 – 8633

**Improvement of output beam quality in broad area lasers with
off-axis feedback**

Mark Lichtner, Vasile Tronciu¹, Andrei Vladimirov¹

submitted: June 20, 2011

¹ Weierstrass Institute
Mohrenstr. 39
10117 Berlin, Germany
E-Mail: lichtner@gmx.net
E-mail: Vasile.Tronciu@wias-berlin.de
E-mail: Andrei.Vladimirov@wias-berlin.de

No. 1615
Berlin 2011



2010 *Mathematics Subject Classification.* 78A60 37M05 78A45.

2008 *Physics and Astronomy Classification Scheme.* 42.55.Px 42.60.Mi 42.60.Da 42.65.Sf.

Key words and phrases. Broad area semiconductor laser, off-axis feedback, supermode.

Edited by
Weierstraß-Institut für Angewandte Analysis und Stochastik (WIAS)
Leibniz-Institut im Forschungsverbund Berlin e. V.
Mohrenstraße 39
10117 Berlin
Germany

Fax: +49 30 2044975
E-Mail: preprint@wias-berlin.de
World Wide Web: <http://www.wias-berlin.de/>

Abstract

We report a method to improve the beam quality of broad area lasers by using a V-shaped external cavity formed by two off-axis feedback mirrors that allow to select a single transverse mode with the intensity modulated in the transverse direction. We find that in the case when one of the two feedback mirrors is absent a spontaneous formation of self-induced transverse population grating leading to a reduction of the lasing threshold is observed. Most favorable conditions for stabilization of single transverse supermode and creation of a high power and high brightness plane wave traveling in the extended cavity are obtained for equal reflectivities of the two external reflectors.

1 Introduction

During recent years high power laser diodes attract much attention because of their applications in material processing, spectroscopy and medicine. Such lasers reach electro-optical efficiencies of more than 70% [1], feature small physical sizes combined with high reliability. Moreover, these devices can exhibit output powers of more than 20 W [2] as single emitters and several hundred Watts when they are combined in laser bars [3]. However, they are known to have a poor beam quality and large slow axis far-field divergence primarily due to filamentation that arises at sufficiently high pump levels. In addition, by lack of spectral filtering they usually operate in unwanted dynamic periodic or chaotic states. To overcome these deficiencies and increase the beam quality and brightness of high power laser diodes several approaches have been proposed. Promising designs are distributed-feedback tapered master oscillators power amplifiers [4, 5] or DBR tapered lasers [6, 7, 8]. They consist of a narrow ridge waveguide for lateral mode filtering and a tapered amplifier integrated on a single chip.

Another approach to improve the beam quality of Broad Area Lasers (BAL) is to apply a filtered feedback from an external cavity [9, 10, 11, 12, 13, 14, 15, 16]. However, most results reported in the literature on BALs with external cavity are purely experimental and lacking a deeper theoretical explanation. In order to fill this gap, in this paper we perform theoretical investigations of a BAL with a tilted, V-shaped external cavity, see Fig. 1. The tilted feedback enforces a spatial phase coupling between different points in the laser transverse section. As it is demonstrated below, this coupling selects and stabilizes a single transverse supermode and creates a high power, high brightness plane wave traveling in the extended cavity. In Section 2, we introduce an appropriate model to describe the laser behavior. To analyze the high power operation regimes in BALs with a strong off-axis filtered optical feedback we have performed a comprehensive time domain numerical modeling taking into account diffraction, gain dispersion, and carrier diffusion in semiconductor medium.

In section 3 we discuss both the non-striped and striped array diode lasers with off axis filtered feedback from a single external mirror. We investigate devices with the same width and length within the same external cavity and compare the results. We demonstrate a formation of a weak periodic transverse modulation of field intensity (antiphase synchronized “emitters”) in the BAL.

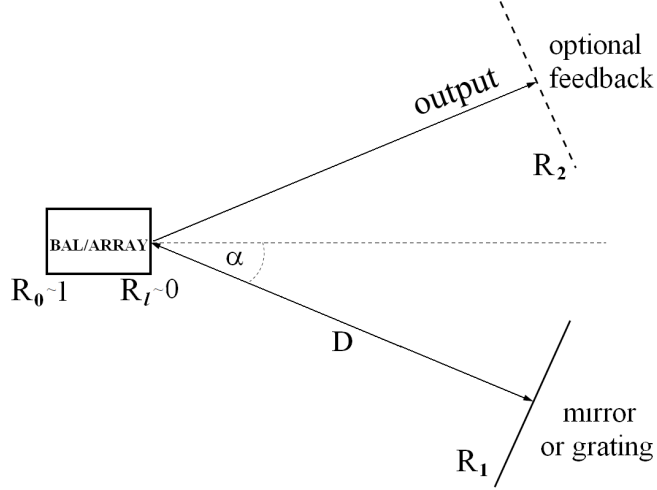


Figure 1: Broad area laser with off axis feedback (V-shaped external cavity).

These oscillations appear due the interference between the waves reflected from the feedback mirror and the left laser facet and the waves scattered by the spontaneously induced population grating in the transverse direction. Such self-organized multi-emitter grating establishes the laser resonator by itself. Section 4 presents an explanation of the farfield asymmetry. In section 5, we apply additional (second) feedback at the opposite flipped angle, i.e. we add the optional upper mirror shown by dashed line in Fig. 1, and find the formation of a transverse periodic pattern resulting from the interference of the plane waves reflected from the two feedback mirrors. This shows that inside a V-shaped cavity the BAL automatically creates its own stripe emitters and can be considered as a self-organized laser array [17]. This demonstrates that the filamentation, which is known to degrade the beam quality of high power tapered lasers [4, 5, 6, 7, 8], can be effectively suppressed in a BAL by imposing a suitable spatial phase coupling due to external off-axis feedback. We also investigate the influence of the spectral filter on the self organization BAL dynamics. By applying suitable spectral filtering (Bragg grating) in the external cavity, the BAL can be operated CW with a single stable antiphase synchronized “multi-emitter” supermode. The antiphase synchronization of the neighboring self-organized “emitters” produces a sharp double lobed far field as does the stripe contacted array. spacing of two longitudinal modes of the external cavity. This longitudinal periodic pulse dynamics is accompanied by lateral periodic collective oscillations of the self-organized stripes inside the BAL. Finally, the summary and conclusions are given in Section 6.

2 The model and parameters.

To model the laser devices shown in Fig. 1 we use the following traveling wave equation equations (1) for the complex slowly varying amplitudes u^\pm of the forward and backward propagating optical fields, coupled to differential equations (2) for the complex slowly varying amplitudes p^\pm of the induced polarization and a parabolic diffusion equation (3) for the real excess carrier

density N :

$$\frac{n_g}{c_0} \partial_t u^\pm = \frac{-i}{2k_0 \bar{n}} \partial_{xx} u^\pm + (\mp \partial_z - i\beta) u^\pm - \frac{\bar{g}}{2} (u^\pm - p^\pm) + F_{\text{sp}}^\pm \quad (1)$$

$$\partial_t p^\pm = \bar{\gamma} (u^\pm - p^\pm) + i\bar{\omega} p^\pm \quad (2)$$

$$\partial_t N = D_N \partial_{xx} N + \frac{J}{qd} - R(N) - \frac{c_0}{n_g} \Re \sum_{\nu=\pm} u^{\nu*} [g(N, u) u^\nu - \bar{g}(u^\nu - p^\nu)] \quad (3)$$

with reflecting boundary conditions at both the left and right facet of the BAL at $z = 0$ and $z = l$, and optical feedback from the external cavity at the right facet $z = l$

$$\begin{cases} u^+(t, x, 0) = \sqrt{R_0(x)} e^{i\varphi_0(x)} u^-(t, x, 0) \\ u^-(t, x, l) = \sqrt{R_l(x)} e^{i\varphi_l(x)} u^+(t, x, l) + u_{FB}(t, x). \end{cases}$$

Here, $t \in \mathbb{R}$ denotes time, $z \in [0, l]$ corresponds to the longitudinal propagation direction, $x \in \mathbb{R}$ to the lateral space dimension of the BAL. $R_l \ll 1$ since the BAL is antireflection coated at the right facet. Feedback from a single tilted external cavity is modeled via

$$u_{FB}(t, x_0) = \sqrt{\frac{1}{i\lambda_0 2D}} e^{-i2\pi \frac{2D}{\lambda_0}} \int_{-\infty}^{\tau} \int_{-\frac{w}{2}}^{\frac{w}{2}} \rho(\tilde{t} - \tau) u^+(t - \tau + \tilde{t}, x, l) e^{-i2\pi \sin(\alpha) \frac{x_0 + x}{\lambda_0}} dx d\tilde{t}. \quad (4)$$

Here D is the distance from the center of the right facet to the grating or mirror, which is assumed to be very large, $D \gg w/2$, α is the angle of the tilt, and $\tau = 2D/c_0$, where c_0 is the light velocity in vacuum. The space integral corresponds to a Fresnel integral and time integration with the kernel $\rho(t) = \sqrt{\Gamma/\pi} \exp(-\Gamma t^2)$ is performed for spectral filtering, see Fig. 1. Γ is the spectral filtering width.

Equation (1) can be derived from the scalar wave equation by using a slowly varying forward and backward rotating wave Ansatz, paraxial approximation, and the effective index method [18]. Equation (2) is a time domain description of a Lorentzian gain dispersion profile [19], and (3) follows from a standard carrier transport equation. All quantities are averaged along the transverse direction perpendicular to the layers.

The factor β is a complex propagation parameter modeled via

$$\beta = \delta_0(x, z) + \delta_n(x, z, N) + i \frac{g(x, z, N, u) - \alpha(x, z)}{2},$$

where g denotes peak gain, depending on the carrier inversion $N = N(t, x, z)$ within the active zone, $\delta_0(x, z)$ is a built-in variation of the dielectric function, independent of N and the

Table 1: Main parameters used in simulations

Symbol	Description	Unit	Value
D	external feedback distance	m	$39 \cdot 10^{-3}$
α	external feedback angle	$grad$	2.8
R_1	external feedback reflectivity		0.99
\bar{n}	reference refractive index		3.27
$g'(x, z)$	differential gain		
	$(x, z) \in \{\text{array}\}$	m^{-1}	2400
	$(x, z) \in \text{elsewhere}$	m^{-1}	0
$\alpha_l(x, z)$	internal absorption		
	$(x, z) \in \{\text{array}\}$	m^{-1}	100
	$(x, z) \in \{\text{PA, elsewhere}\}$	m^{-1}	0
N_{tr}	transparency carrier density	m^{-3}	$1.3 \cdot 10^{24}$
l_a	length of array	m	$5 \cdot 10^{-3}$
w_a	array width	m	$4 \cdot 10^{-6}$
d	thickness of active region	m	$16 \cdot 10^{-9}$

temperature, whereas δ_n describes the dependence of the effective refractive index on N , which is responsible for electrical lensing and filamentation. We use the following models for g and δ_n :

$$g = g(x, z, N, u) = g'(x, z) \frac{\ln(N(t, x, z)/N_{tr})}{1 + \epsilon(|u_+|^2 + |u_-|^2)}, \quad (5)$$

$$\delta_n(x, z, N) = -k_0 \sqrt{n'(x, z)N(t, x, z)}. \quad (6)$$

The function $J(x, z)$ denotes the injection current density, so that the injection I is given by $I = \iint J(x, z) dx dz$.

The model equations are solved numerically with the help of the software developed at WIAS [20]. To discretize the model equations we use a splitting scheme, in which diffraction and the carrier diffusion in the lateral direction are resolved by means of fast Fourier transform, while the remaining coupled hyperbolic system is integrated along characteristics of Eq. (1) using finite differences. We have assumed a central wavelength $\lambda_0 = 976$ nm and a group refractive index $n_g = 3.66$. Other parameters as listed in Table 1. In addition, we neglect heating effects. A more detailed explanation of all parameters can be found in, e.g., [5]. Finally we note that the model was verified experimentally in previous papers [17, 8, 5].

3 BALs with off axis feedback

3.1 Stripe array BALs

We start our analysis by considering a 40 emitter striped gain-guided BAL array with single tilted feedback mirror [17], see Fig. 1. The stripes having a width of 4 microns are separated by passive regions of 6 microns width. Thus the array period is $d = 10$ microns (see Fig. 2 a). Unlike globally coupled laser arrays which can exhibit inphase synchronization of individual emitters (see e.g. [21, 22, 23]) with a single lobe far field pattern, in the presence of weak local coupling between the emitters via evanescent fields they naturally either operate in antiphase regime [24] or demonstrate complicated dynamical regimes. In the case of antiphase synchronization two lobes dominate in the far field output field radiating at angles $\pm\alpha$, where

$$|\alpha| \sim \sin(|\alpha|) = \frac{\lambda_0}{2d}. \quad (7)$$

To enhance the antiphase coupling of the stripes we set the feedback angle to α (or more precisely $-|\alpha|$). Thus a transverse optical supermode with intensity maxima located on top of

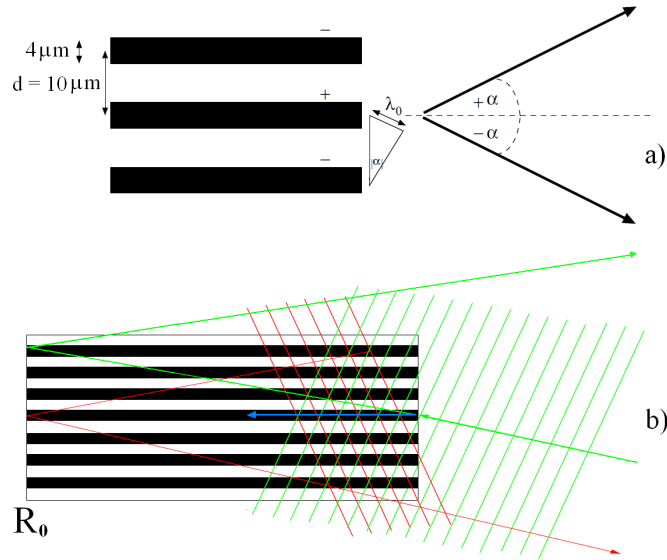


Figure 2: Schematic view of stripe array. a) Antiphase synchronized BAL stripe array with two preferred output angles given by (7). b) Plane wave scattering on the transverse grating introduced by the stripe array.

each stripe (see Fig. 3 a) is stabilized. This supermode corresponds to a plane wave traveling to the mirror and reflected back to the BAL array. The striped array can be considered as a gain and index grating in the transverse direction. Hence a part of the plane wave with positive transverse wavenumber traveling from the feedback mirror to the left laser facet is scattered by the grating into a wave with negative transverse wavenumber, see Fig. 2 b). After reflection from the left facet R_1 , the latter wave returns back to the feedback mirror. Similarly the plane wave with the positive wavenumber reflected from the left facet is scattered into a wave with

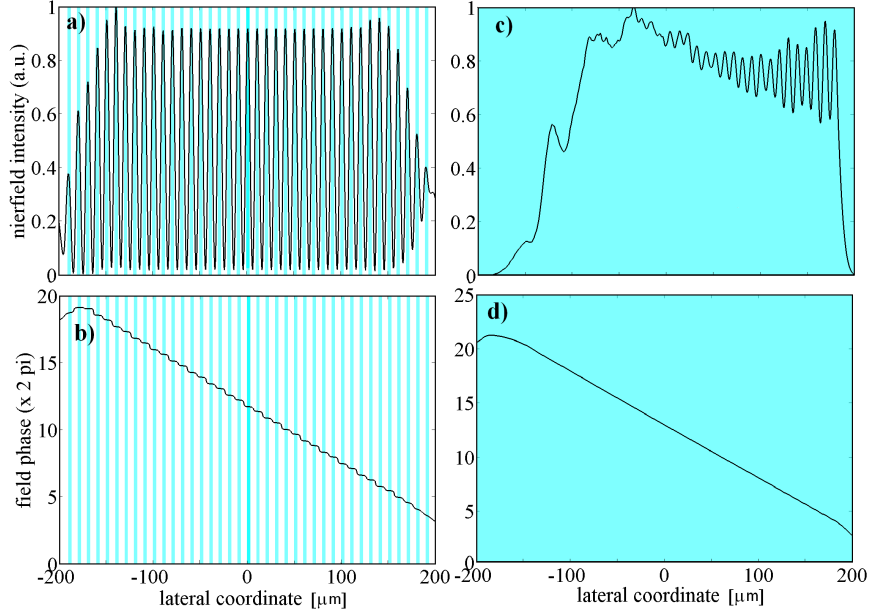


Figure 3: Near field intensity for a) 40 striped BAL laser array and c) for nonstriped BAL. Near field phases in the bottom panels b) and d) correspond to the intensity distribution shown in the top panels. Grey (cyan) area are pumped stripes. The injected current is fixed to 12 A. Other parameters are as in Table 1.

negative transverse wavenumber traveling in the direction of the feedback mirror. The panel (b) in Fig. 3 shows computed near field phases of the laser array. Each stripe is phase locked and neighboring stripes are antiphase. We note that in [17] we have shown that for twice higher feedback angles a stable supermode exists with twice the number of emitters with intensity maxima not located on top of each stripe (every second intensity maximum located between two adjacent stripes).

3.2 Weak self organization in nonstriped BALs

In the previous section, we have clarified some aspects of the behavior of a striped BALs. In what follows, we are interested in the self-organization of nonstriped BALs. Let us now consider a nonstriped BAL of the same size as the stripe array placed into the external cavity with the same feedback angle $-|\alpha|$. Since the striped gain grating is missing now one would not expect to have additional waves scattered on this grating, see Fig. 2 b). Instead a unidirectional light propagation is expected, where the plane wave traveling from the feedback mirror is reflected out at the left laser facet R_1 at the angle $+|\alpha|$. Nevertheless, as it is seen from Fig. 3 c) and d), the computed nearfield of the nonstriped BAL also exhibit a weak periodical modulation of the electric field intensity at positive lateral coordinates. The distance d between neighboring field maxima can be considered as the distance between the effective “emitters”. It can be tuned by adjusting the feedback angle α . While the striped array is stabilized mainly by gain guiding the formation of the self induced “emitters” in the transverse section of BAL can be explained by electronic self-focusing (modeled by equation (6)) and feedback (modeled by Eq. (4)).

According to the panel (d) in Fig. 3, neighboring intensity maxima have opposite phases similarly as in the stripe array. However, in contrast to the array, which has a lateral step-like change of the optical field phase (see panel (b) of Fig. 3), the near-field phase of the BAL changes almost linearly with the averaged slope determined by the feedback mirror tilt angle α . This nearly uniform rotation of the near field phase, which corresponds mainly to a single outgoing plane wave, is represented also by the theoretical far field (lower panel in Fig. 4) with an almost complete suppression of the feedback lobe at the angle $-|\alpha|$.

Thus, by self-organization a weak population grating is created in the laser medium, which (together with the left laser facet) acts as an effective mirror that reflects a small part of the plane wave traveling from the feedback mirror in the opposite direction. This allows a considerable reduction of the lasing threshold and, hence, an achievement of laser generation. However, due to the weakness of the self-induced grating, the laser threshold still remains much higher than that in the striped array. This can be seen by the high noise level in Fig. 3 c). The tiny internal reflectivity is indicated by the almost disappearance of the feedback lobe compared to the output lobe in the lower panel of Fig. 4. This asymmetry is explained in the next section.

4 Explanation of the farfield asymmetry

Fig. 4 shows the farfield of the striped laser array. We observe the usual double lobed narrow far field pattern with a slightly suppressed feedback lobe at $-|\alpha|$ and a pronounced output lobe at $+|\alpha|$, in agreement with the common experimental results, see for example [10, 17].

On the contrary, the farfield of the BAL shown in the lower panel of Fig. 4, has almost no feedback lobe. This can be explained by the weakness of the self-induced transverse grating in the BAL. The tiny modulation amplitude of the transverse intensity distribution shown in the lower panel of Fig. 4 implies small periodic oscillations in the carrier density distribution due to spatial hole burning. This, according to Eqs. (5)-(6), creates a weak gain and index grating. For the device with a V-shaped resonator shown in Fig. 1 we derive a simple mathematical relation which gives the ratio of the output and feedback lobe field amplitudes. Let us denote $|E_{1,2}^-|^2$ ($|E_{1,2}^+|^2$) the stationary electric field intensities of the plane wave traveling from the mirror 1 (2) to the mirror 2 (1) evaluated at these mirrors. Here the index 1 (2) corresponds to lower (upper) mirror. Similarly $|E_0^\pm|^2$ denote the intensities of the two counter-propagating plane waves incident at the left laser facet with the reflectivity R_0 . Assuming that reflectivity of the right laser facet vanishes, $R_l = 0$, we write the following relations between the above mentioned intensities

$$|E_0^-|^2 = \sqrt{r}e^{G/2} \left[(1 - \kappa) |E_1^-|^2 + \kappa |E_2^+|^2 \right] \quad (8)$$

$$|E_2^-|^2 = R_0 \sqrt{r}e^{G/2} \left[(1 - \kappa) |E_0^-|^2 + \kappa |E_0^+|^2 \right], \quad (9)$$

and

$$|E_0^+|^2 = \sqrt{r}e^{G/2} \left[(1 - \kappa) |E_2^+|^2 + \kappa |E_1^-|^2 \right] \quad (10)$$

$$|E_1^+|^2 = R_0 \sqrt{r}e^{G/2} \left[(1 - \kappa) |E_0^+|^2 + \kappa |E_0^-|^2 \right], \quad (11)$$

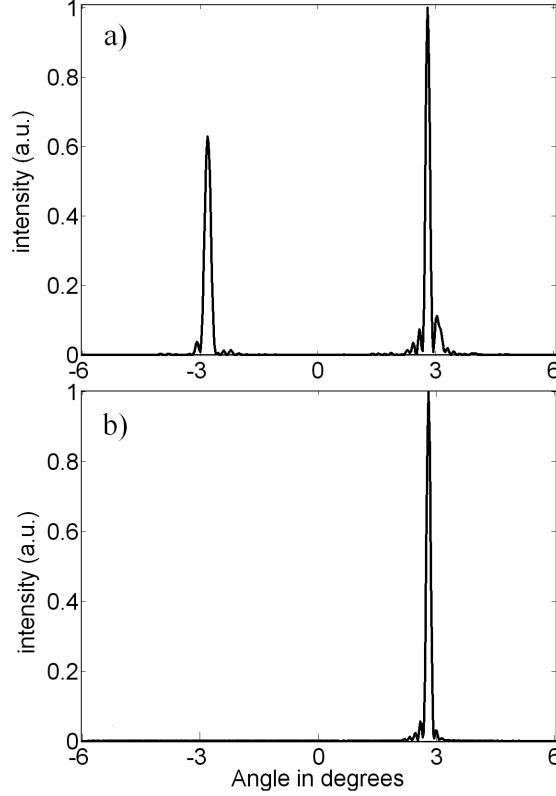


Figure 4: Far field for a) 40 striped BAL laser array and b) nonstriped BAL.

Here $e^G > 1$ and $r < 1$ are, respectively, amplification and attenuation factors per cavity round trip and κ describes the fraction of energy scattered by the transverse grating into the wave with opposite transverse wavenumber. The boundary conditions at the mirrors 1 and 2 read

$$|E_1^-|^2 = R_1 |E_1^+|^2, \quad |E_2^+|^2 = R_2 |E_2^-|^2. \quad (12)$$

From the solvability condition of Eqs. (8)-(12) we get the following relation for the amplification factor per cavity round trip:

$$e^G = \frac{1}{rR_0} \left\{ \kappa(1 - \kappa)(R_1 + R_2) + \sqrt{[R_1\kappa^2 + R_2(\kappa - 1)^2][R_1(\kappa - 1)^2 + R_2\kappa^2]} \right\}^{-1}, \quad (13)$$

$$\frac{|E_1^+|^2}{|E_2^-|^2} = \frac{1}{(1 - \kappa)^2 + \kappa^2} \left\{ \kappa(1 - \kappa) \left(1 - \frac{R_2}{R_1} \right) + \sqrt{\left[(1 - \kappa)^2 + \kappa^2 \frac{R_2}{R_1} \right] \left[\frac{R_2}{R_1} (1 - \kappa)^2 + \kappa^2 \right]} \right\} \quad (14)$$

In particular, since in the absence of the upper mirror self-induced grating is weak ($\kappa \ll 1$), for

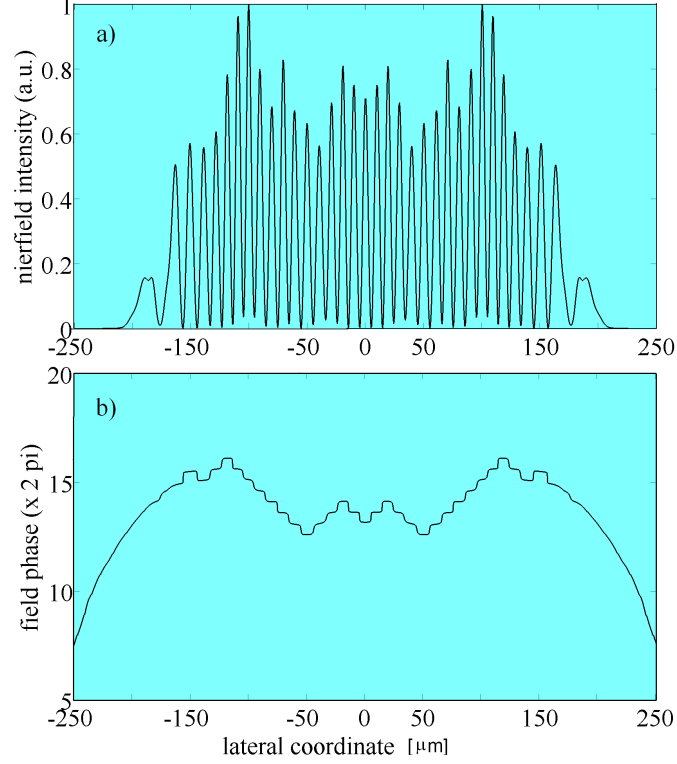


Figure 5: a) Self organized emitters (nearfield) in a BAL with symmetric feedback and b) corresponding near field phases. The parameters are as in Fig. 3 a).

$R_2 = 0$ we obtain

$$\frac{|E_1^+|^2}{|E_2^-|^2} = \frac{2(1-\kappa)\kappa}{(1-\kappa)^2 + \kappa^2} \approx 2\kappa \ll 1, \quad (15)$$

On the other hand, for $\kappa = 0$ we get

$$\frac{|E_1^+|^2}{|E_2^-|^2} = \sqrt{\frac{R_2}{R_1}}, \quad (16)$$

Finally the ratio of the field intensities emitted from the two feedback mirrors is given by

$$\frac{|E_1^{out}|^2}{|E_2^{out}|^2} = \frac{(1-R_1)|E_1^+|^2}{(1-R_2)|E_2^-|^2}, \quad (17)$$

It follows from Eqs. (14)-(17) that the ratio $|E_1^{out}/E_2^{out}|^2$ and, hence, the amplitude E_1 vanishes in the limit $R_2, \kappa \rightarrow 0$. This result is in agreement with Fig. 4, where the output field peak is much larger than the feedback one. According to Eq. (13) in the absence of transverse grating ($\kappa = 0$) the generation cannot be achieved in a BAL with a single feedback mirror, $R_2 = 0$. In this case the lasing threshold becomes infinite. However, even small population grating results in the backscattering from the BAL to the lower mirror: this results in shifting the laser threshold to finite values of injection current $e^G = [2r\kappa(1-\kappa)R_0R_1]^{-1}$.

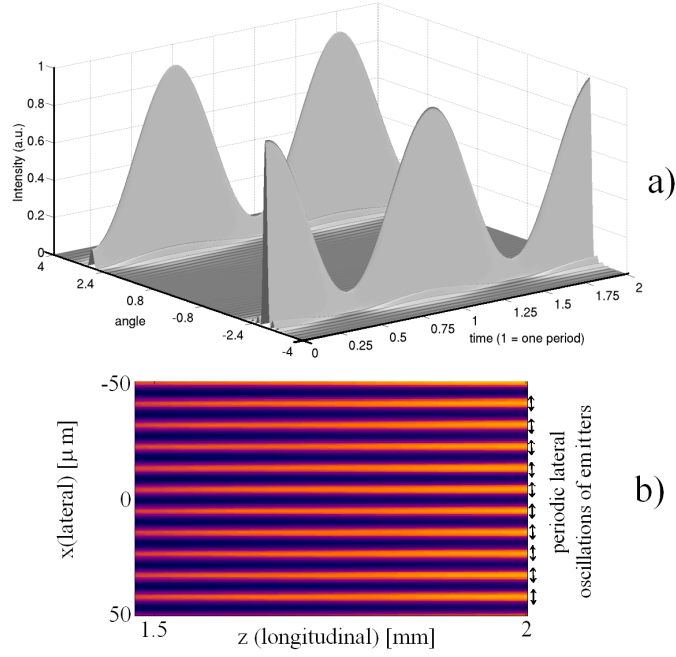


Figure 6: a) Periodic antiphase pulsation of the output intensities in the case when spectral filter selects two longitudinal cavity modes. b) Periodic lateral movements of self organized emitters.

5 Dynamic self organization of BALs with second feedback

The characteristics of the with single tilted feedback BAL with tiny self organized internal reflectivity can be improved by adding a second feedback at the flipped angle $+|\alpha|$. Let us consider the same BAL as in section 3.2 but with two feedback mirrors placed symmetrically and including the optional grating, see Fig. 1. Computed nearfield pattern is shown in Fig. 5. A supermode with nearly the same number of self organized emitters as in the stripe array in Fig. 3 a) is visible because the lateral width of the BAL was chosen equal to the width of the stripe array. The amplitudes of the periodic nearfields are, however, nonhomogeneous in contrast to the stripe array in Fig. 3 a). One observes an amplitude envelope with two pronounced ears towards the border. For sufficiently narrow spectral filter, which selects one longitudinal mode of the full cavity (which has a length of $8cm$) we find the laser in single CW supermode operation. Applying nonsymmetric feedback only perturbs the stripe supermode (it remains stable in time and space) in such a way that the nearfield intensity increases towards the output branch with smaller feedback. By increasing the spectral width of the filter multimode pulsations appear. These pulsations are accompanied with a lateral spatial dynamics of the self organized stripes. Fig. 6 a) shows the far field evolution of a two mode pulsation. The antiphase intensity oscillations in Fig. 6 a) are accompanied with a periodic $\pm 2\mu m$ lateral movement of the self organized stripes shown in Fig. 6 b). When the pulse is crossing the BAL gain medium and is traveling towards the down (top) mirror, it is amplified so that higher nearfields are obtained at down (top) coordinates. Due to spatial hole burning this on average implies a decreasing (increasing) carrier distribution. Hence the stripe supermode gets more gain when it moves up (down) if the pulse is traveling to the down (up) mirror. This can also be expressed by decomposing the supermode in two active

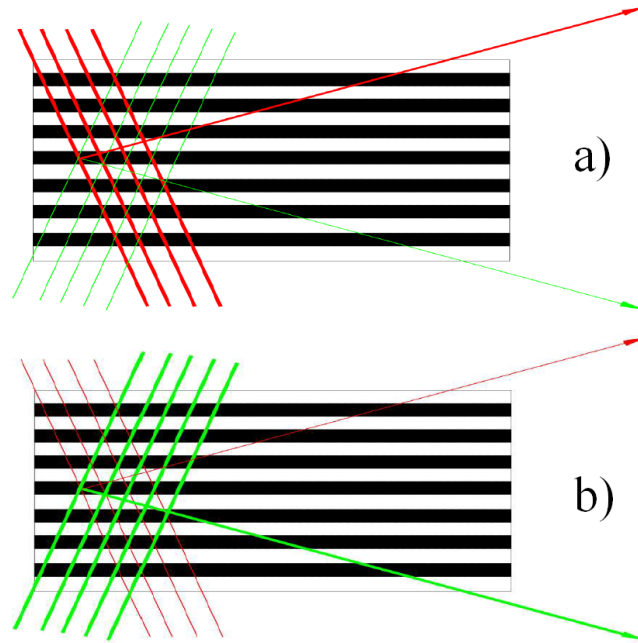


Figure 7: Schematic view of the creation of supermodes. a) top supermode, b) down supermode.

up and down radiating supermodes. The lateral stripe movements then correspond to periodic relative phase oscillations of the two supermodes, see Fig. 7.

6 Conclusions

We have studied a method for improving the beam quality of broad area lasers by using a feedback from an external cavity. We have considered both the case of a striped laser array and non-striped BAL subjected to a feedback from either a single tilted mirror or a pair symmetrically tilted mirrors forming a V-shaped cavity. In the case of non-striped BAL with a single feedback mirror we have demonstrated a formation of a weak periodic transverse modulation of the field intensity. This self-organized multi-emitter grating is responsible for a scattering leading to an energy exchange between the waves with opposite transverse wavenumbers and, hence, for a build up of lasing. The lasing threshold can be considerably reduced by replacing a single feedback mirror with a V-shaped cavity. Such kind of cavity selects four plane waves with opposite transverse and longitudinal wavenumbers and creates a well pronounced stripe emitters in the semiconductor medium due to the interference of these waves. Thus the filamentation can be effectively suppressed in a BAL by imposing a suitable spatial phase coupling due to external off-axis feedback. We have also demonstrated that by applying suitable spectral filtering (Bragg grating) in the external cavity, the BAL can be operated in CW state with a single stable antiphase synchronized “multi-emitter” supermode. By increasing the width of the spectral filtering a high power periodic pulse is traveling in the full cavity with frequency given by the intermode spacing of two longitudinal modes of the external cavity. Finally, using the model and theoretical analysis we were able to explain the farfield asymmetry in nonstriped BALs. We believe that

our work provides a good basis for future studies and, in particular, some pointers for more detailed investigations of broad area lasers containing V-shaped external cavity and its practical applications.

7 Acknowledgments

AGV acknowledges the support from the SFB 787 of the DFG, EU FP7 Marie Curie Initial Training Network, Grant No. 264687, and the Programme "Research and Pedagogical Cadres for Innovative Russia," grant 2011-1.5-503-002-038.

References

- [1] M. Kanskar, T. Earles, T.J. Goodnough, E. Stiers, D. Botez, and L.J. Mawst, *Electron. Lett.* 41, 245 (2005).
- [2] K. J. Paschke, S. Einfeldt, A. Ginolas, K. Haeusler, P. Ressel, B. Sumpf, H. Wenzel, and G. Erbert, in *CLEO/QELS 2008 Conference Digest p. CMN4* (2008).
- [3] H. Li, I. Chyr, X. Jin, F. Reinhardt, T. Towe, D. Brown, T. Nguyen, M. Berube, T. Truchan, D. Hu, et al., *Electron. Lett.* 43, 27 (2007).
- [4] H. Wenzel, K. Paschke, O. Brox, F. Bugge, J. Fricke, A. Ginolas, A. Knauer, P. Ressel, and G. Erbert, *Electron. Lett.* 43, 160 (2007).
- [5] M. Spreemann, M. Lichtner, M. Radziunas, U. Bandelow, and H. Wenzel, *IEEE J. Quantum Electron.* 45, 609 (2009).
- [6] K.-H. Hasler, B. Sumpf, P. Adamiec, F. Bugge, J. Fricke, P. Ressel, H. Wenzel, G. Erbert, and G. Trankle, *Photonics Technology Letters* 20, 1648 (2008).
- [7] C. Fiebig, G. Blume, C. Kaspari, D. Feise, J. Fricke, M. Matalla, W. John, H. Wenzel, K. Paschke, and G. Erbert, *Electronics Letters* 44, 1253 (2008).
- [8] C. Fiebig, V. Z. Tronciu, M. Lichtner, K. Paschke, and H. Wenzel, *Applied Physics B* 99, 209 (2010).
- [9] A. Jechow, V. Raab, and R. Menzel, *Appl. Opt.* 47, 1447 (2008).
- [10] B. Thestrup, M. Chi, and P. M. Petersen, *Proc. SPIE* 5336, 3844 (2004).
- [11] S. Wolff, A. Rodionov, V. Sherstobitov, and H. Fouckhardt, *IEEE J. Quantum Electron.* 39, 448 (2003).
- [12] L. Lang, J. J. Lim, S. Sujecki, and E. C. Larkins, *Opt. Quantum Electron.* 40, 1097 (2008).
- [13] M. Chi, B. Thestrup, and P. M. Petersen, *Opt. Lett.* 30, 1147 (2005).

- [14] A. Jechow, V. Raab, R. Menzel, M. Cenkier, S. Stry, and J. Sacher, *Opt. Commun.* 277, 161 (2007).
- [15] L. Goldberg and J. Weller, *Electron. Lett.* 25, 112 (1989).
- [16] K. Iida, H. Horiuchi, O. Matoba, T. Omatsu, T. Shimura, and K. Kuroda, *Opt. Commun.* 146, 6 (1998).
- [17] A. Jechow, M. Lichtner, R. Menzel, M. Radziunas, D. Skoczowsky, and A. G. Vladimirov, *Optics Express* 17, 19599 (2009).
- [18] S. Balsamo, F. Sartori, and I. Montrosset, *IEEE Journal of Selected Topics in Quantum Electronics* 2, 378 (1996).
- [19] U. Bandelow, M. Radziunas, J. Sieber, and M. Wolfrum, *IEEE J. Quantum. Electron.* 37, 183 (2001).
- [20] M. Lichtner and M. Spreemann, *WIAS-preprint* 1326, 1 (2008).
- [21] G. Kozyreff, A. G. Vladimirov, and P. Mandel, *Phys. Rev. Lett.* 85, 3809 (2000).
- [22] G. Kozyreff, A. G. Vladimirov, and P. Mandel, *Phys. Rev. E* 64, 16613 (12 pages) (2001).
- [23] A. Vladimirov, G. Kozyreff, and P. Mandel, *Europhysics Letters* 61, 613 (2003).
- [24] R. Li and T. Erneux, *Optics Communications* 99, 196 (1993).